



Contents lists available at ScienceDirect

Journal of Molecular Liquids

journal homepage: www.elsevier.com/locate/molliq

Kinetic investigations on alkaline fading of malachite green in the presence of micelles and reverse micelles

Q1 Somnath Dasmandal, Harasit Kumar Mandal, Arjama Kundu, Ambikesh Mahapatra*

Department of Chemistry, Jadavpur University, Kolkata 700 032, India

ARTICLE INFO

Article history:

Received 29 July 2013

Received in revised form 7 October 2013

Accepted 12 December 2013

Available online xxxx

Keywords:

Hydrolysis

CMC

Water pool

Emission spectroscopy

Tensiometry

Thermodynamic parameters

ABSTRACT

The kinetics of alkaline hydrolysis of malachite green (MG^+) have been studied spectrophotometrically in the presence of cetyltrimethylammonium bromide (CTAB) under pseudo-first-order condition at buffered of pH 11 and 298 K. The rate increases slightly up to the critical micelle concentration of CTAB then increases rapidly for surface catalysis of the micelles. The reaction has also been studied in the water pools of the CTAB/1-butanol/heptane/water reverse micelles and found 4–8 times faster over its rate in aqueous phase but the rate decreases exponentially with its water pool (w) size. The CTAB micellar medium has been characterized using steady state emission spectroscopy and tensiometry at the reaction condition for better explanation of the experimental findings. The thermodynamic activation parameters for the hydrolysis reaction have also been determined for comparison of the kinetic behavior in different environments.

© 2013 Elsevier B.V. All rights reserved.

1. Introduction

The chemistry of dyes and their applications to other scientific fields get immense popularity in the modern era. They have played an important role as an effective indicator in the analysis of some elements such as ruthenium (Ru), iodine (I) and osmium (Os) [1]. The recognition of DNA by dye molecules is of paramount importance in biochemistry and molecular biology [2]. Dye sensitization of semiconductors is becoming a promising strategy for solar energy conversion [3]. The principal application of dyes is in the coloration of substrates, typically textiles, where a great quantity of water and dyes are used, with about 50% of the dyes discharged into wastewater, thereby polluting the environment [4]. The wastewater, discharged from textile industries, contains high concentrations of reactive dyes that exert serious threats to sustainability of natural ecosystems [5]. Moreover, the contamination of reactive dyes may present a risk to the aquatic living organisms through bioaccumulation thus entering into their food chain. Toxicity of reactive dyes has been reported at concentrations as low as 5.2 mg L^{-1} [6]. Recently, several methods for dealing with the treatment of textile wastewater like physico-chemical treatment [5], biological oxidation [7], adsorption and advanced oxidation processes (AOPs), e.g. ozonation, photolysis, electrochemical, and sonolysis [8] have been investigated. Usually, these processes lead to the release of more toxic products than the parent compound that prove fatal for the living

creatures [9]. Hydrolysis is one of the prime detoxification mechanisms for organic compounds as hydrolysis by-products are normally less toxic to the environment than the parent compound [10].

A number of investigations over the last three decades [11–13] have revealed that the rates of a variety of organic reactions are altered in the presence of dilute aqueous solution of surfactants [14]. One of the most important properties of the aqueous surfactant solution is their ability to solubilize a wide variety of organic molecules, thereby influencing their reactivity. The variation of rate can be explained with the specific interactions between surfactant molecules and reactant species, viz. Coulombic, hydrophobic and charge transfer. All of the interactions can play a significant role in altering the rate of the reaction [15,16]. The surfactant molecules mutate the reaction rate through the formation of aggregates, called micelles. These micelles are capable in changing the rate of the reaction by several ways [17]—decreasing the entropy of reactant species due to their binding with micelles, relative stabilization or destabilization of the reactants due to their preferential interaction with surfactants and promoting the approach of reactants towards the micellar core. The catalytic activity of micelles has been studied for different organic reactions, especially the hydrolysis of esters [18], Schiff bases and carbocationic dyes [19]. That means the micellar effects on the reactivity have frequently been a matter of study. However, a lot of interests have been placed on the study with reverse micelles because of its similarity with the microenvironment in the biological cells [20]. Although the majority of kinetic studies have been carried out in the ternary systems formed by AOT (sodium bis(2-ethylhexyl) sulfosuccinate)/alkane/water microemulsions [21]; nevertheless, only few systematic quantitative studies have been carried out in four component microemulsions [22–24]. Zakharova et al. [25] have shown

* Corresponding author. Tel.: +91 33 2457 2767 (office), +91 33 2432 4586 (residence); fax: +91 33 2414 6223.

E-mail addresses: amahapatra@chemistry.jdvu.ac.in, ambikeshju@gmail.com (A. Mahapatra).

the catalytic effect of reverse micellar systems on the alkaline hydrolysis of phosphonic acid esters. Microemulsions, also called reverse micelles, are pseudo-heterogeneous mixtures of water-insoluble organic compounds, water and a surfactant/co-surfactant mixture. They are transparent, isotropic and thermodynamically stable dispersion systems of 'oil' and 'water'. Two types of reverse micelles are recognized—oil-in-water (*o/w*) reverse micelles, where the 'oil' resides at the center of the droplet and is surrounded by surfactant and co-surfactant, whereas 'water' is at the droplet center in the water-in-oil (*w/o*) reverse micelles. The size of liquid drop in the dispersed phase is in the range of 8–80 nm. Due to the dynamic nature of reverse micelles, they can exchange their constituents including water, surfactants or other content [26]. The charged head groups of the reverse micelles make the liquid confined in it different in their physical properties from that of the bulk phase [27,28]. The liquids, entrapped in a very small cavity of nanometer range, play the fundamental role as a medium that controls the structures, functions and thermodynamics of the system which is akin to that of the biological membrane system. One of the most striking features of reverse micelles is the "water pool" which is usually expressed by the molar ratio of water to surfactant i.e., $w = [\text{H}_2\text{O}]/[\text{Surf.}]$ [29–31]. The size of water pool can precisely be controlled by taking different values of 'w'. The parameter 'w' is believed to be the key factor in controlling the most important structural features of the reverse micellar system. In most instances, water-in-oil systems (*w/o*) have been used and the water droplets have been proven useful as 'minireactors' for various types of reactions.

Malachite green (di[4-dimethylaminophenyl]phenyl cation) is an important water soluble dye. The name of the dye just comes from the similarity of its color. These dyes represent a class of dyes of commercial and analytical importance [32]. The high solubility of the dye in water makes it potential water pollutants. In the textile industry, the removal of the dyes from effluents in an economic fashion is a major problem. Since these wastewaters contain substances that modify the medium, and a study of the dyes fading in the presence of surfactants, which are already present in such water, can contribute to the development of new decontaminating procedures. The kinetic studies of alkaline fading of malachite green thus have extensively been developed [33].

In this article, we have presented some of our interesting results on the study of kinetics of alkaline fading of malachite green in micellar medium and reverse micellar medium of the cationic surfactant CTAB. All of the experimental works have been carried out in buffer medium of pH = 11 at 298 K. The reaction of malachite green with hydroxide ions is a one-step reaction [34] and follows pseudo-first-order kinetics. Rationalizations of the kinetic results with proper explanations have been attempted.

2. Experimental

2.1. Reagents & materials

Malachite green (MG^+), CTAB, sodium carbonate and bicarbonate salts have been used as received from Merck, India. Pyrene has been procured from Sigma-Aldrich and used without further purification. N-Cetyl pyridinium chloride (CPC) has been purchased from Merck, India and recrystallized from methanol/ethanol mixture before use. Highly pure water from Milli-Q Ultra has been used for preparation of aqueous solutions throughout the experiment. Fresh aqueous solution of malachite green has been used for day to day works and it is stored in a dark place. The concentration of malachite green solution has been determined spectrophotometrically using its molar extinction coefficient, $\epsilon_{616}(\text{MG}^+) = 148424 \text{ L mol}^{-1} \text{ cm}^{-1}$ [35]. The aqueous solution of CTAB and CPC have been prepared with $0.02 \text{ mol L}^{-1} \text{ Na}_2\text{CO}_3 = 0.02 \text{ mol L}^{-1} \text{ NaHCO}_3$ buffer solution of pH = 11 (± 0.02). Ethanolic solution of pyrene has been used as a probe. All fluorimetric, tensiometric and kinetic experiments have been carried out at a constant temperature of 298 K and buffer medium of pH = 11.

2.2. Methods

2.2.1. Fluorimetry

Steady-state fluorescence measurements have been performed on a Shimadzu RF-5000 spectrofluorimeter thermostated at 298 K ($\pm 0.1 \text{ K}$). For the determination of critical micelle concentration (CMC) and effective dielectric constant (ϵ) on CTAB micellar surface, a pyrene solution of concentration $1 \times 10^{-6} \text{ mol L}^{-1}$ has been used as a probe. Pyrene has been excited at 332 nm, and its emissions recorded at 375 and 386 nm corresponding to the first and third vibronic peaks respectively, with the use of both excitation and emission slits of 5 nm. The formation of micelle has been attributed by the change in the intensity ratios of the first and third peaks ($I_{\text{I}}/I_{\text{III}}$) from the emission spectra of pyrene. The aggregation number (N) of CTAB in buffer (pH = 11) medium has been determined using the steady-state fluorescence quenching (SSFQ) method where N-Cetyl pyridinium chloride (CPC) has been employed as quencher (Q). For the determination of N , the concentration of CTAB has been kept well above its CMC throughout the experiments.

2.2.2. Tensiometry

Tensiometric measurement has been carried out on a calibrated du Nouy tensiometer (Jencon, India) employing ring detachment technique [36]. A buffer solution of 10 mL has been placed in a thermostated 298 K ($\pm 0.1 \text{ K}$) double walled jacketed glass container where the CTAB solution of desired concentration has been added gradually in a number of steps with the aid of a micro-pipette from Finnpiptette. After each addition of surfactant, the mixture has been stirred well using a magnetic stirrer, allowed the mixture to equilibrate and finally the measurement of surface tension (γ) was carried out subsequently. The measured values of surface tension have been found to be reproducible within $\pm 0.02 \text{ dyn cm}^{-1}$.

2.2.3. Kinetic measurements

The alkaline hydrolysis reactions have been carried out spectrophotometrically on a UV-visible Spectrophotometer (Shimadzu, UV-1800) equipped with a Peltier temperature controller, TCC-240A maintaining a constant temperature of 298 K ($\pm 0.1 \text{ K}$). The kinetics of hydrolysis reactions have usually been performed up to 2–3 half-lives of the reaction. The decrease in absorbance (Fig. 1) at 616 nm has been recorded as a function of time. All the kinetic runs have been carried out under pseudo-first-order conditions with excess amount of alkali over MG^+ . The observed pseudo-first-order rate constants (k_{obs}) have been

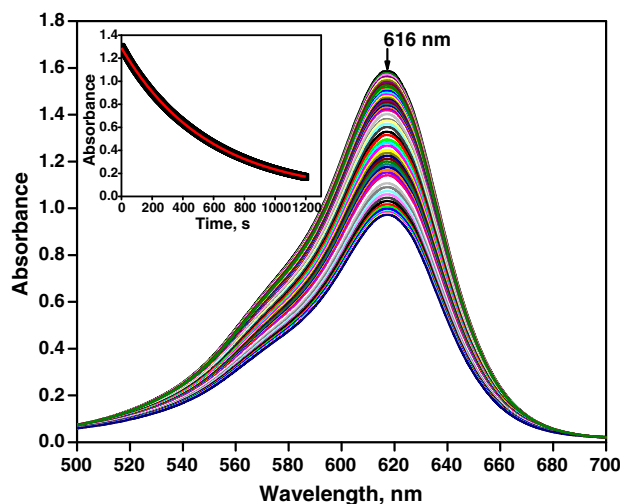


Fig. 1. UV-vis Spectra of MG^+ and ^-OH reaction mixture in an aqueous buffer medium at different time intervals. [Inset: Change of absorbance as a function of time at 616 nm.] $[\text{MG}^+]_0 = 5.77 \times 10^{-5} \text{ mol L}^{-1}$, pH = 11, $\mu = 4 \times 10^{-3} \text{ mol L}^{-1}$ at 298 K.

determined from the first order exponential decay curve fitting of absorbance (A_t) against time (t) graph using Microcal Origin 8.0 software on a computer.

Microemulsions of desired compositions have been prepared by the addition of appropriate volume of aqueous part (MG^+ and buffer). Thus the concentrations of MG^+ inside the water pool i.e., the local concentration of MG^+ ($[\text{MG}^+]_L$) have been calculated considering the total volume of the added aqueous part.

3. Results and discussion

3.1. Fluorimetry

3.1.1. Determination of CMC and micellar surface effective dielectric constant (ϵ) of CTAB

The fluorescence spectrum of pyrene in aqueous solution possesses significant vibronic fine structure consisting of five major peaks. Being a hydrophobic compound, pyrene tends to solubilize in the micellar core of aqueous micellar solutions of CTAB and thereby experiences some variations in its spectrum from that obtained in surfactant solutions of concentrations below CMC. The intensity ratio of the first vibrational band (375 nm), the highest energy one, and the third

vibrational band (386 nm), I_I/I_{III} , have been plotted against surfactant concentration, above and below the CMC (Fig. 2a). The CMC value of CTAB has been obtained from the vicinity of inflection point on the sigmoidal curve. A derivative plot has been used for accurate determination of CMC (Table 1).

The vibronic peak intensity ratio (I_I/I_{III}) in the pyrene emission spectrum provides a measure of the apparent environmental micropolarity as this ratio is directly related to the dielectric constant where the probe is housed [37]. An increment in the intensity ratio is the indication of increased polarity. The result shows the intensity ratio decreases sharply with surfactant concentration closes to the CMC. It indicates that micellar surface becoming less polar as the concentration of surfactant increases. This ratio (I_I/I_{III}) becomes constant at 1.34 when the concentration of CTAB is sufficiently greater than CMC. The effective dielectric constant of the micellar surface has been estimated from the calibration plot between fluorescence intensity ratio (I_I/I_{III}) and static dielectric constant (ϵ) of various solvents [38] and the value has come out as 42.5 (Fig. 2b).

3.1.2. Determination of aggregation number (N)

The micellar aggregation number has been obtained from fluorescence quenching measurements where the probe (pyrene) and the quencher have been assumed to be solubilized on the micellar pseudo phase [39]. The ratio of the intensities in the absence of quencher (I_0) to that in the presence of quencher, I_0/I , is related to the quencher concentration by Eq. (1) [40]

$$\ln \frac{I_0}{I} = \frac{N[Q]}{\text{CMC} - [S]_T} \quad (1)$$

where, $[Q]$ is the total concentration of the quencher, $[S]_T$ and CMC are the total concentration and critical micelle concentration of CTAB respectively. The aggregation number (N) at different surfactant concentrations has been obtained from the slope of the plot of $\ln(I_0/I)$ versus $[Q]$ (Fig. 3) and the values have been shown in Table 2. The aggregation number of CTAB micelles in aqueous buffer medium (pH = 11) has been found to increase continuously in the concentration range of $(3-30) \times 10^{-3} \text{ mol L}^{-1}$ [41] which eventually means the increment of micellar surface area with the increase of surfactant concentration.

3.2. Tensiometry

The surface tension of CTAB has been found to decrease rapidly with the addition of surfactant, and it remains almost unchanged after the onset of micellization even if the concentration of surfactant has been further increased. The CMC value has easily been obtained from the intersection of two straight lines of the plot of surface tension (γ) versus the logarithmic surfactant concentration ($\log \{[\text{CTAB}]_0/\text{mol L}^{-1}\}$) (Fig. 4). The value of CMC obtained in this technique (Table 1) is in good agreement with that obtained by fluorimetric measurements.

3.3. Kinetics

3.3.1. Effect of malachite green on the rate of reaction

The solution of malachite green consists of a colored cation (MG^+) of which the intense color is due to the presence of conjugation in the

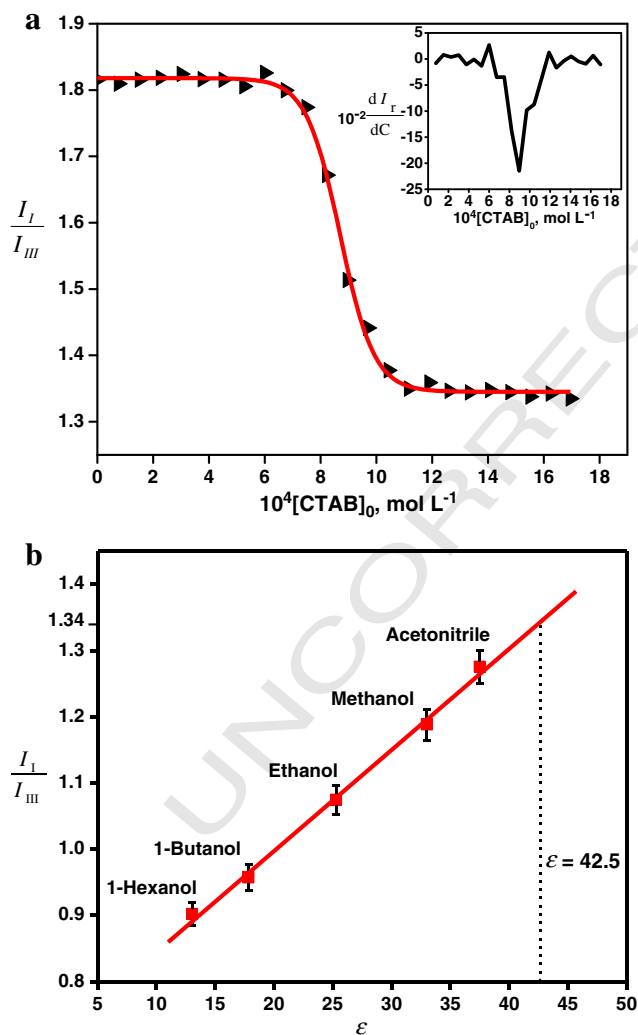


Fig. 2. a Fluorescence intensity ratio of pyrene vibronic peaks I_I and I_{III} , (I_I/I_{III}) versus $[\text{CTAB}]_0$ [I_I and C in the inset stand for I_I/I_{III} and $[\text{CTAB}]_0$ respectively.] $[\text{Py}]_0 = 1 \times 10^{-6} \text{ mol L}^{-1}$, pH = 11 at 298 K. b Calibration plot of fluorescence intensity ratio of pyrene vibronic peaks I_I and I_{III} , (I_I/I_{III}) versus static dielectric constant (ϵ) of commonly used solvents. $[\text{Py}]_0 = 1 \times 10^{-6} \text{ mol L}^{-1}$, pH = 11 at 298 K.

Table 1

Critical micelle concentration (CMC) of aqueous solution of CTAB (pH = 11) in different techniques at 298 K.

Technique	$10^3 \text{ CMC, mol L}^{-1}$	
Spectrofluorimetric	0.87 ± 0.02^a	t1.5
Tensiometric	0.86 ± 0.02^a	t1.6
Kinetic	0.82 ± 0.02	t1.7

^a CMC value has been lowered considerably from that of reported value in pure water [42] by both fluorimetry and tensiometry methods.

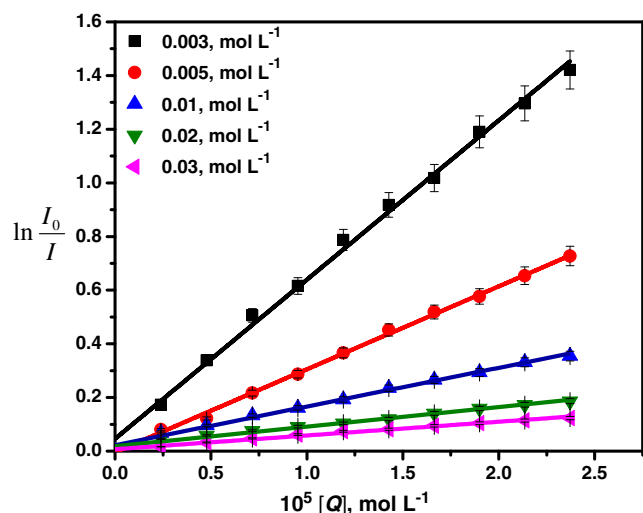


Fig. 3. Natural logarithm of pyrene fluorescence intensity ratio, $\ln(I_0/I)$ versus quencher concentrations, $[Q]$ at different initial concentrations of CTAB. $[Py]_0 = 1 \times 10^{-6} \text{ mol L}^{-1}$, $\text{pH} = 11$ at 298 K.

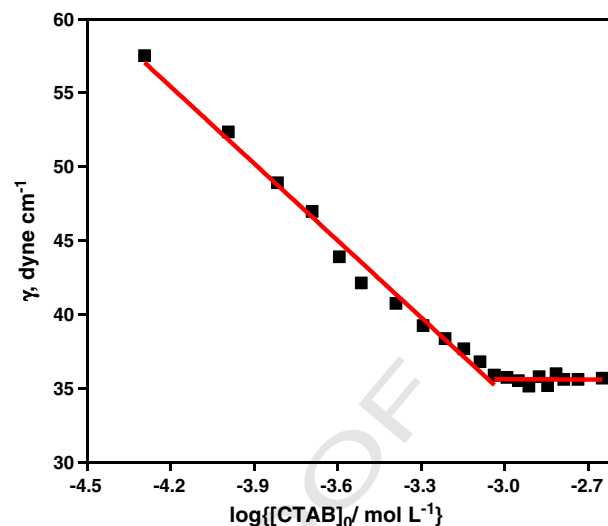


Fig. 4. Variation of the surface tension (γ) with logarithm of CTAB concentration at $\text{pH} = 11$ and 298 K.

system. The alkaline hydrolysis of MG^+ results in a disruption of the conjugation and consequent loss of the color with time. The reaction proceeds according to Scheme 1.

The kinetic studies has been carried out keeping the concentration of MG^+ very low compared to that of OH^- in order to maintain the pseudo-first-order condition. Under this circumstance, a series of kinetic runs have been carried out in the range of concentration of MG^+ $(1.15\text{--}8.63) \times 10^{-5} \text{ mol L}^{-1}$ at constant excess concentration of hydroxide ion ($[\text{OH}^-]_0 = 1.0 \times 10^{-3} \text{ mol L}^{-1}$) at 298 K. The ionic strength (μ) of the medium has been maintained at $4.0 \times 10^{-3} \text{ mol L}^{-1}$ by adding NaNO_3 .

The absorbance of MG^+ (at 616 nm) has been found to decay exponentially with time. The plot of observed pseudo-first-order rate constant, k_{obs} , versus $[\text{MG}^+]_0$ shows that the values of k_{obs} remain almost constant $\{(1.89 \pm 0.03) \times 10^{-3} \text{ s}^{-1}\}$ upon changing the concentration of MG^+ which confirms the first-order dependence of reaction rate on the concentration of MG^+ .

3.3.2. Effect of hydroxide on the rate of reaction

A few kinetic runs for the alkaline hydrolysis of malachite green have been performed with the variation of $[\text{OH}^-]_0$ in the range of $0.2\text{--}2.0 \text{ mol L}^{-1}$ at $[\text{MG}^+]_0 = 5.77 \times 10^{-5} \text{ mol L}^{-1}$, $\mu = 4.0 \times 10^{-3} \text{ mol L}^{-1}$ at 298 K. The values of k_{obs} obtained at different $[\text{OH}^-]_0$ $\{(0.57\text{--}3.32) \times 10^{-3} \text{ s}^{-1}\}$, reveal a linear dependence on $[\text{OH}^-]_0$ indicating that the reaction is first-order with respect to the concentration of OH^- . The well known mechanism of this reaction taking place in bulk phase [43] has been presented in Scheme 1. The observed rate law can be expressed as

$$\text{rate} = -\frac{d[\text{MG}^+]}{dt} = \{k_0 + k_{\text{OH}}[\text{OH}^-]_0\} [\text{MG}^+]_0.$$

Table 2
Micellar Aggregation numbers for different initial concentrations of CTAB ($\text{pH} = 11$) at 298 K.

$10^3 [\text{CTAB}]_0 \text{ mol L}^{-1}$	Aggregation number (N) ^a
3.0	124
5.0	126
10.0	130
20.0	138
30.0	147

^a Aggregation numbers have been calculated from Eq. (1) using CMC value of $0.87 \times 10^{-3} \text{ mol L}^{-1}$.

Under the experimental condition, $[\text{OH}^-]_0 \gg [\text{MG}^+]_0$ i.e., the initial concentration of OH^- remains almost constant throughout the reaction. Therefore,

$$-\frac{d[\text{MG}^+]}{dt} = k_{\text{obs}} [\text{MG}^+]_0 \quad (2)$$

where,

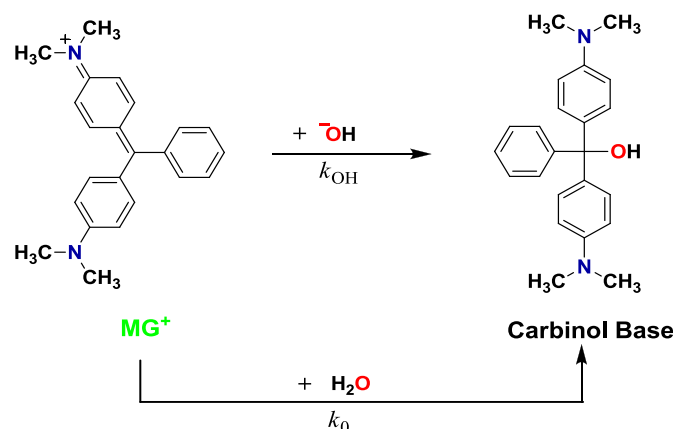
$$k_{\text{obs}} = k_0 + k_{\text{OH}}[\text{OH}^-]_0$$

k_{OH} is the second-order rate constant for alkaline hydrolysis reaction. Here, the value of the rate constant for hydrolysis of MG^+ in pure water, k_0 , has been obtained from the intercept of the plot k_{obs} versus $[\text{OH}^-]_0$ and it comes out as $2.9 \times 10^{-4} \text{ s}^{-1}$. The value of k_{OH} calculated from Eq. (2) is $1.51 \pm 0.04 \text{ L mol}^{-1} \text{ s}^{-1}$.

All other experimental works have been performed with a particular initial concentration of hydroxyl ion (i.e., $1.0 \times 10^{-3} \text{ mol L}^{-1}$) which has been obtained by using a buffer of $\text{Na}_2\text{CO}_3\text{--NaHCO}_3$. However, in this circumstance, the requisite pseudo-first-order condition has still been maintained and also the reaction shows first-order kinetics with respect to $[\text{OH}^-]_0$.

3.3.3. Influence of CTAB on the rate of reaction

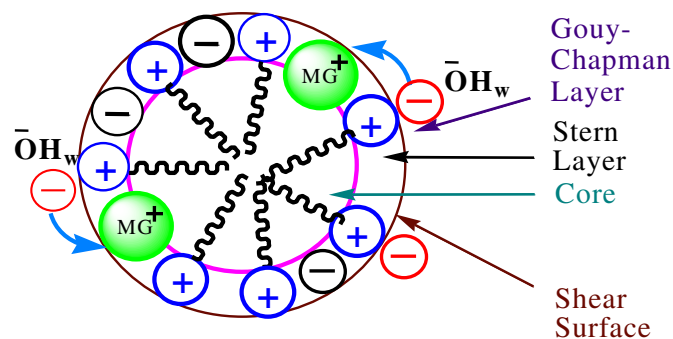
We have examined the influence of cationic surfactant, CTAB, on the alkaline hydrolysis of malachite green (MG^+) throughout the pre- and



Scheme 1. Hydrolysis of Malachite Green (MG^+).

306 post-micellar region. Observed pseudo-first-order rate constants (k_{obs})
 307 for hydrolysis of MG^+ at constant $[^-OH]_0$ have been found to increase
 308 by nearly 7 times with an increase in the total concentration of CTAB
 309 from 0.0 to $5.4 \times 10^{-3} \text{ mol L}^{-1}$. The rate of the process has initially
 310 been found to increase slightly, but after a certain concentration of sur-
 311 factant it rises much steeply up to a limit beyond which the increment of
 312 the rate is not too much (Fig. 5). The critical micelle concentration
 313 (CMC) of CTAB has been obtained kinetically as the minimum surfactant
 314 concentration required inducing a substantial change in the observed
 315 rate constant. The obtained value, $CMC = 0.82 \times 10^{-3} \text{ mol L}^{-1}$, is
 316 somewhat smaller (~25%) than the value obtained tensiometrically in
 317 pure water, $1.09 \times 10^{-3} \text{ mol L}^{-1}$ (very close to the reported value
 318 [42]), which has been ascribed to the known effect of the presence of
 319 electrolytes on the critical micelle concentration of surfactant. This
 320 value of CMC obtained kinetically has been observed in good agreement
 321 with that obtained in tensiometric and fluorimetric measurements
 322 (Table 1).

323 In post-micellar region, the catalytic effect of CTAB is a result of the
 324 increased local concentration of the reactants in the micellar pseudo
 325 phase [44]. It has been found that the aggregation number of CTAB mi-
 326 celles increases steadily with CTAB in the concentration range of
 327 $(3.0\text{--}30.0) \times 10^{-3} \text{ mol L}^{-1}$ (Table 2). The availability of surface area
 328 of the micelles thus increased with the addition of CTAB which in conse-
 329 quence increases the effective concentrations of MG^+ and ^-OH ions in
 330 the Stern layer due to hydrophobic (as the organic moieties are present
 331 in malachite green) and Coulombic interaction respectively (Scheme 2),
 332 and thereby increasing the reaction rate. It has already been shown that
 333 the dielectric constant of MG^+ micro-environment decreases with CTAB
 334 concentration. This decrease in the effective dielectric constant (ϵ) has
 335 been attributed to the creation of electric field by the charged micelle
 336 surface [45]. The value of ϵ obtained on CTAB micellar surface,
 337 42.5 (at 298 K), is much smaller than that in aqueous phase, $\epsilon = 80.1$
 338 ($I_1/I_{III} \approx 1.81$) [38] According to Hughs–Ingold rule [46,47] for nucleo-
 339 philic substitution reactions, the formation of the neutral carbinol base
 340 (Scheme 1) from two oppositely charged reactants is more favorable
 341 in lower dielectric constant media and thus with increase in CTAB con-
 342 centration, the rate of alkaline fading of MG^+ increases. However, the
 343 rate of the reaction at sufficiently high concentration of CTAB
 344 ($\gg CMC$) has been found to be almost constant due to the increased
 345 Coulombic repulsion between the micellar head groups and MG^+
 346 which prevents the further incorporation of MG^+ into the micellar core.



Scheme 2. Schematic representation of CTAB micelle with embedded reactant molecules on micellar surface.

347 The effect of micellar systems on chemical reactions has been ex-
 348 plained quantitatively in terms of the micellar pseudo phase (PP)
 349 model [48]. The variation of the rate constant (k_{obs}) with surfactant
 350 concentration has been treated as shown in Scheme 3.

351 The substrate MG^+ has been assumed to bind with n number of sur-
 352 factant molecules with binding constant $K_{MG^+}^m$ to form aggregates and k_w^h
 353 & k_m^h are the pseudo-first-order rate constants for the alkaline hydrolysis
 354 in the aqueous medium, and micellar pseudophases respectively. This
 355 model leads to the following expression of k_{obs} for micelle-catalyzed
 356 reaction. The detailed derivation of k_{obs} has been shown in supplement-
 357 ary data.

$$k_{obs} = \frac{k_w^h + k_m^h K_{MG^+}^m \left(\frac{[D]}{C^0}\right)^n}{1 + K_{MG^+}^m \left(\frac{[D]}{C^0}\right)^n} \quad (3)$$

358 where C^0 is the standard concentration. The experimental results have
 359 been fitted to Eq. (3) by means of a non-linear regression analysis
 360 using Origin 8.0 (Fig. 5). The value of k_{OH} has been kept constant and
 361 is equal to the value previously obtained in aqueous phase. The values
 362 of the rate constants (k_{obs} and k_{cal}), $K_{MG^+}^m$ and k_m^h for CTAB micelles
 363 have been summarized in Table 3. The observed value of n (Table 3)
 364 is far less than the number of surfactant molecules found in the micelle
 365 (Table 2). This has been interpreted as indicative of the formation of
 366 small sub-micellar aggregates which interacts with the reactants and
 367 thereby increases the rate, though slightly, at surfactant concentration
 368 below the CMC.

3.3.4. Influence of CTAB reverse micelles on the rate of reaction

370 The study has been carried out on the influence of microemulsion
 371 composition on the rate of alkaline hydrolysis of malachite green
 372 in two ways—variation of the size of water pools keeping the concen-
 373 tration of CTAB fixed and also varying the CTAB concentration at
 374 constant w .

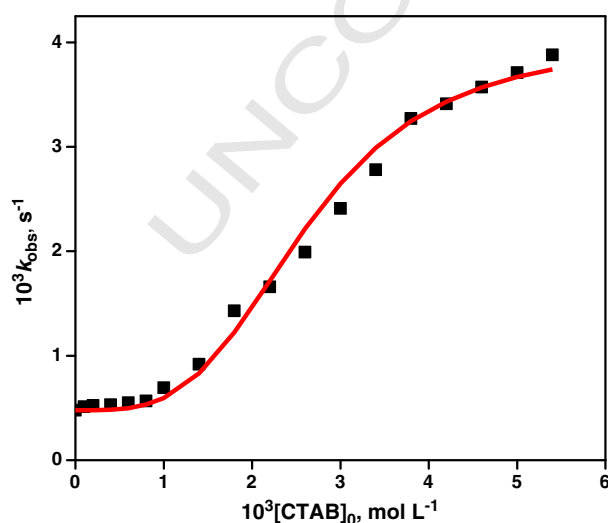
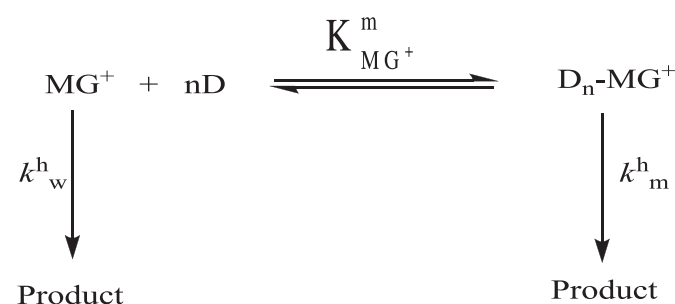


Fig. 5. Effects of $[CTAB]_0$ on pseudo-first order rate constants (k_{obs}) for hydrolysis of MG^+ . $[MG^+]_0 = 5.77 \times 10^{-5} \text{ mol L}^{-1}$, pH = 11 at 298 K.



Scheme 3.

Table 3
Pseudo-first-order rate constants (k_{obs} and k_{cal}) for alkaline hydrolysis of MG^+ in CTAB micellar medium at 298 K.

$10^3 [\text{CTAB}]_0$ mol L ⁻¹	$10^3 k_{\text{obs}}$ (s ⁻¹)	$10^3 k_{\text{cal}}$ (s ⁻¹)	$10^3 k_{\text{m}}^{\text{h}}$ (s ⁻¹)	$K_{\text{MG}^+}^{\text{m}}$	$n (\pm 0.2)$
0.0	0.48	0.48			
0.1	0.51	0.48			
0.2	0.52	0.48			
0.4	0.53	0.48			
0.6	0.55	0.50			
0.8	0.57	0.53			
1.0	0.69	0.58			
1.4	0.92	0.80			
1.8	1.43	1.17	4.01	9.6×10^8	3.5
2.2	1.66	1.65			
2.6	1.99	2.15			
3.0	2.41	2.60			
3.4	2.78	2.97			
3.8	3.27	3.25			
4.2	3.41	3.45			
4.6	3.57	3.61			
5.0	3.71	3.72			
5.4	3.88	3.80			

The microemulsions are assumed to be divided into three regions—the oil-rich domain (o); the central aqueous core (w) and the surfactant interfacial region (i). The reactants distribute themselves among the three pseudophases according to their solubilities, and the overall rate of the reaction would be the sum of the rates in the different pseudophases.

3.3.4.1. Identification of the reaction position. The observed experimental behavior can be interpreted by acquiring the knowledge of the location of both reactants in the microemulsion. Under the conditions of this study, the hydrolysis reactions may take place either in the aqueous pseudophase (i.e., aqueous core) or at the interface or both according to the distribution of the reactants. The OH^- ions are highly hydrophilic in nature and their suitable location should be in the aqueous pseudophase of the microemulsion, whereas the Coulombic repulsion between malachite green (MG^+) and CTAB head groups will compel the dye to be present in the water rich domain i.e., inside the water pool, whether a portion of MG^+ may also be present at the interface due to hydrophobic interaction with CTAB. The hydrolysis reactions are therefore assumed to be occurring primarily in the central aqueous core of the microemulsion, although a small part of the reaction seemed to be taking place at the interface.

Therefore, the mechanistic Scheme 4 (a) can be simplified to Scheme 4 (b). On the basis of this diagram, the reaction rate can be expressed as,

$$r = k_w[S]_w + k_i[S]_i \quad (4)$$

where $[S]_w$ & $[S]_i$ are the molar concentrations of MG^+ in central aqueous core and at the interface respectively and k_w & k_i are the true hydrolysis rate constant in the central aqueous core and at the interface respectively.

Let $r = r_1 + r_2$, where, $r_1 = k_w[S]_w$ and $r_2 = k_i[S]_i$
As $[S]_w \gg [S]_i$
i.e. $r_1 \gg r_2$
So, $r_1 + r_2 \approx r_1$.

Therefore, Eq. (4) has been reduced to

$$r = k_w[S]_w \quad (5)$$

The distribution equilibrium of the substrate between the surfactant interfacial region and the aqueous pseudophase can be defined in terms of molar relation such as

$$K_{\text{iw}} = \frac{[S]_w}{[S]_i} w \quad (6)$$

Considering that the total concentration of the substrate (MG^+) would be the sum of the concentrations in the two pseudophases i.e., $[S]_t = [S]_w + [S]_i$ applying Eqs. (5) and (6), the expression of k_{obs} can be formulated as

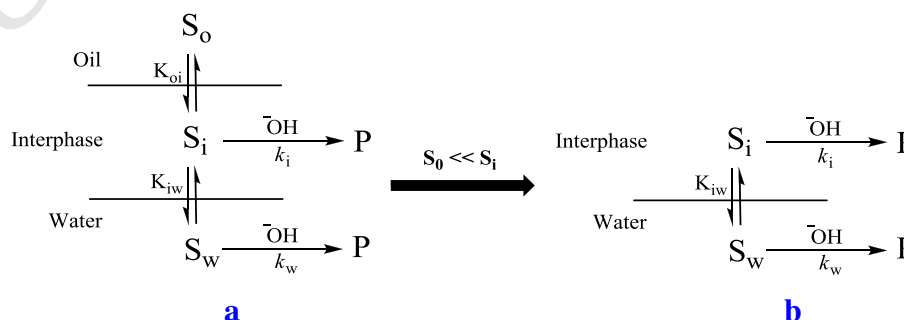
$$k_{\text{obs}} = \frac{k_w K_{\text{iw}}}{K_{\text{iw}} + w} \quad (7)$$

Eq. (7) can be rearranged as

$$\frac{1}{k_{\text{obs}}} = \frac{1}{k_w} + \frac{1}{k_w K_{\text{iw}}} w \quad (8)$$

Eq. (7) predicts the existence of a linear relationship between $1/k_{\text{obs}}$ versus w . Fig. 6 reveals the expected linear dependency of k_{obs} on w indicating the reaction to be occurring in the central aqueous core of the microemulsion. The values of k_w and K_{iw} obtained from the intercept and the slope of the curve have been tabulated in Table 4.

3.3.4.2. (a) Influence of the size of water pool (w). The kinetics of alkaline hydrolysis of malachite green (MG^+) have been studied in a series of experiments in which the size of water pools have been varied



Scheme 4. (a) Probable distributions of MG^+ among the pseudophases of CTAB reverse micelle & (b) identification of the position of hydrolysis reaction.

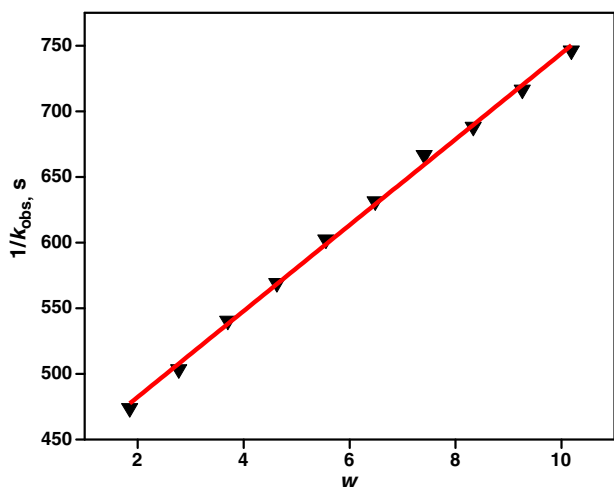


Fig. 6. Variation of $1/k_{obs}$ with the size of water pools (w) in CTAB/1-butanol/heptane/water reverse micelle. [CTAB] = 0.1 mol L^{-1} , pH = 11 at 298 K.

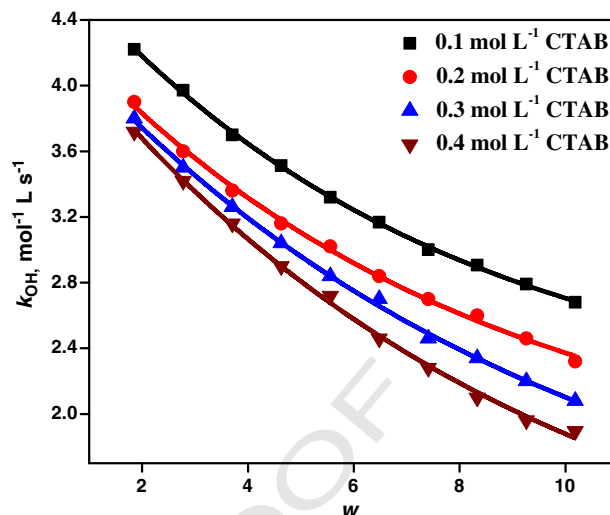


Fig. 7. Variation of k_{OH} with the size of water pools (w) in CTAB/1-butanol/heptane/water reverse micelle at different initial concentrations of CTAB. $[MG^+]_L = 8.65 \times 10^{-4} \text{ mol L}^{-1}$, pH = 11 at 298 K.

432 ($w = 1.852\text{--}10.185$) keeping the concentration of CTAB constant. The
 433 experimental results show an exponential decrease in the values of
 434 second-order rate constant (k_{OH}) upon increasing the size of water
 435 pools (w) (Fig. 7). In CTAB reverse micelles, the water dipoles are
 436 strongly oriented by the counter ions, Br^- , present inside the central
 437 aqueous core [49]. The hydrogen bonds among the water molecules
 438 thus get destroyed partially. Therefore, the effective concentration of
 439 ^-OH ions can be expressed as

$$[^-OH]_e = \frac{n^-OH}{V_w^f} \quad (9)$$

440 We know that,

$$V_w = V_w^f + V_w^b \quad (10)$$

443 where, n^-OH is the no. of moles of ^-OH ions, V_w is the total volume of
 445 water added, V_w^f and V_w^b are the volumes of free water and that of
 446 bound water respectively. As the orientation of bound water is restricted
 447 by Br^- ions, it would not take part into solvation of the reactant spe-
 448 cies. It is obvious that V_w^b is proportional to the no. of moles of CTAB
 449 present in the system. Therefore,

$$V_w^b \propto [CTAB] \quad (11)$$

450 where b is a constant, related to the quantity of bound water in CTAB re-
 452 verse micellar system.

453 Using Eqs. (10) and (11) we have

$$V_w^f = V_w(1 - b/w) \quad (12)$$

454 **Table 4**
 44.1 K_{iw} values for the distribution of MG^+ between interface and central aqueous core of
 44.2 reverse micelle for different initial concentrations of CTAB at 298 K.^a

44.4	[CTAB] ₀ , mol L ⁻¹	10 ³ k_{iw} , s ⁻¹	K_{iw}
44.5	0.1	2.23 ± 0.04 ^b	12.73
44.6	0.2	2.24 ± 0.05	10.91
44.7	0.3	2.38 ± 0.05	8.04
44.8	0.4	2.50 ± 0.05	6.16

44.9 ^a $[MG^+]_L = 8.65 \times 10^{-4} \text{ mol L}^{-1}$, pH = 11.0.

44.10 ^b Error limits are standard deviations.

Therefore from Eq. (9)

$$[^-OH]_e = \frac{n^-OH}{V_w} = \frac{n^-OH}{V_w(1 - b/w)} \quad (13)$$

455 $[^-OH]_{aq}$ is the molar concentration of ^-OH solution used for the prepara-
 456 tion of reverse micelles.

457 Considering the effective concentrations of the reactant species, hydro-
 458 lysis rate inside the water pool can be expressed as

$$r = k[^-OH]_e [MG^+]_e = k_{obs} [MG^+]_e \quad (14)$$

459 The rate constant values used in Fig. 7 have been obtained by divid-
 460 ing the k_{obs} values by the corresponding $[^-OH]_{aq}$ values. Thus,

$$k_{OH} = \frac{k_{obs}}{[^-OH]_{aq}} = \frac{k_{obs}}{[^-OH]_e(1 - b/w)} \quad (15)$$

461 Eq. (15) clearly indicates that the bimolecular rate constant (k_{OH}) for
 462 the hydrolysis reaction in CTAB reverse micelles decreases upon in-
 463 creasing the values of w .

464 The diminishing trend of the rate constant (k_{OH}) in microemulsion
 465 can be attributed to the differences in properties between surfactant-
 466 entrapped water and bulk water. It has been speculated that the water
 467 trapped in microemulsion is less polar than water in the continuous
 468 aqueous phase [50] and decreasing the size of water pools also leads
 469 to a decrease in the polarity of the water within it. This consideration
 470 leads us to investigate the kinetic consequences upon the hydrolysis re-
 471 action occurring in the central aqueous core. As we have stated previ-
 472 ously, Hughs–Ingold rule predicts that the rate of reactions between
 473 two oppositely charged reacting species forming a neutral product is fa-
 474 cilitated on going from more polar medium to a less polar medium. The
 475 alkaline hydrolysis of malachite green leads to the formation of neutral
 476 carbinol base (Scheme 1), which is stabilized in a less polar
 477 environment. This implies k_{OH} decreases along with w . Furthermore,
 478 the local concentrations of the reactants inside the water pool
 479 ($[MG^+]_L$ and $[^-OH]_L$) have been found to be surprisingly high in

Table 5
Second-order rate constants (k_{OH}) at 298 K and the thermodynamic activation parameters for alkaline hydrolysis of MG^+ (pH = 11.0) in different environments.

Medium	k_{OH} , $mol^{-1} L s^{-1}$ (298 K)	$\Delta^\ddagger H^0$, $kJ mol^{-1}$	$\Delta^\ddagger S^0$, $J mol^{-1} K^{-1}$ (298 K)	$\Delta^\ddagger G^0$, $J mol^{-1}$ (298 K)	E_a , $kJ mol^{-1}$ (298 K)
Aqueous ^a	0.47	71 ± 1	-13.0 ± 0.3	75 ± 2	73 ± 2
Micelle ^b	0.69	67 ± 1	-22.9 ± 0.5	74 ± 2	69 ± 1
Reverse micelle ^c	$w = 1.852$	55 ± 1	-50.5 ± 1.0	69 ± 1	57 ± 1
	$w = 5.555$	2.66	57 ± 1	-46.9 ± 0.9	70 ± 1
	$w = 10.185$	1.68	59 ± 1	-43.4 ± 0.8	71 ± 2

^a $[MG^+]_0 = 5.77 \times 10^{-5} mol L^{-1}$
^b $[MG^+]_0 = 5.77 \times 10^{-5} mol L^{-1}$, $[CTAB]_0 = 1.4 \times 10^{-3} mol L^{-1}$
^c $[MG^+]_L = 8.65 \times 10^{-4} mol L^{-1}$, $[CTAB]_0 = 0.4 mol L^{-1}$

comparison with the bulk aqueous phase and this has been reflected in the values of k_{OH} . In our experimental conditions, the rate constant in microemulsion has been found as 4–8 times as in bulk aqueous phase (Table 5). As we vary the size of water pools (w) from 1.852 to 10.185, the effective concentrations of the reactants inside the water pools decrease and k_{OH} get decreased consequently.

3.3.4.3. (b) Influence of the concentration of CTAB. Alkaline hydrolysis of malachite green in CTAB reverse micelle has also been studied with the variation of CTAB in the concentration range of 0.1–0.4 $mol L^{-1}$ for fixed values of w (Fig. 8). From Fig. 8, it has been observed that k_{OH} decreases exponentially with [CTAB]. The experimental results have been interpreted considering the formalism of distribution of a solute between two phases. The cationic dye, malachite green distributes itself both at the interface and in the central aqueous core of the reverse micelles. The values of distribution coefficient, K_{iw} , have been found to decrease as we increase the initial concentration of CTAB (Table 4), that means the effective concentration of MG^+ in the aqueous core decreases. Therefore, the k_{OH} values for the alkaline hydrolysis of MG^+ in the reverse micelles decrease with CTAB at all w values.

3.3.5. Effect of temperature on the rate of reaction

The effect of temperature on the rate of alkaline hydrolysis reaction has been studied in aqueous, CTAB micellar medium and reverse micellar medium at different temperatures in order to obtain the activation parameters of the reactions. The plot of $\ln\{(k_{OH}/T)/mol^{-1} L s^{-1} K^{-1}\}$ versus $1/T$ (Fig. 9) shows that the second order rate constants increase

linearly with temperature as expected from the Eyring–Polanyi equation (Eq. (16)). From the transition state theory, [51]

$$\ln\left(\frac{k_{OH}/T}{mol^{-1} L s^{-1} K^{-1}}\right) = \ln\left(\frac{k_B/h}{K^{-1} s}\right) + \frac{\Delta^\ddagger S^0}{R} - \frac{\Delta^\ddagger H^0}{RT} \quad (16)$$

where the symbols have their usual meanings. If we extrapolate the five lines of Fig. 9 towards higher temperature, it can be found that they will intersect at a single point, corresponding to a temperature of 429.7 K (± 2 K). This temperature is clearly an iso-kinetic temperature, since all the five reactions in different environments must have the same rate constant (k_{OH}) at this point [52].

The values of standard entropy of activation ($\Delta^\ddagger S^0$), standard enthalpy of activation ($\Delta^\ddagger H^0$) and free energy of activation ($\Delta^\ddagger G^0$) of the respective mediums have been determined using Eq. (16) and the calculated values have been tabulated in Table 5. The activation energy (E_a) of the series of reactions has also been determined (Table 5) from Arrhenius plots of $\ln(k_{OH}/mol^{-1} L s^{-1})$ versus $1/T$. The kinetic data indicates that the second order rate constant in different media follows the order: CTAB reverse micellar medium >> CTAB micellar medium >> aqueous medium.

From the data of Table 5 (and Fig. 9), $\Delta^\ddagger H^0$ has been plotted against $\Delta^\ddagger S^0$ (Fig. 10) and the plot shows a linear relationship between $\Delta^\ddagger H^0$ and $\Delta^\ddagger S^0$ according to Eq. (17) for the series of reactions

$$\Delta^\ddagger H_i^0 = \alpha + \beta \Delta^\ddagger S_i^0 \quad (17)$$

where α and β are constants and the quantity β is often defined as the iso-kinetic temperature.

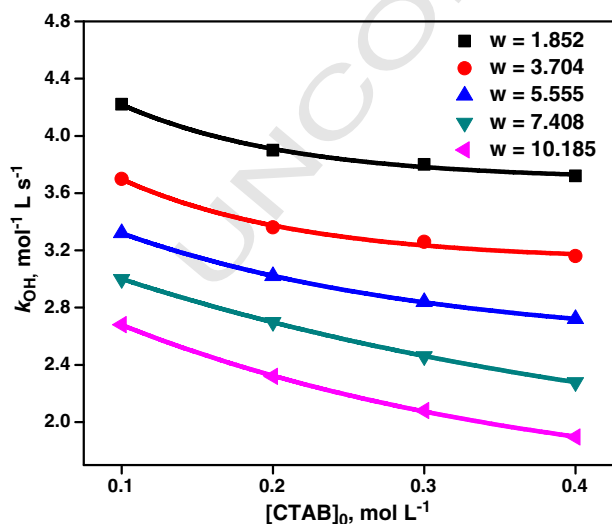


Fig. 8. Second-order rate constant (k_{OH}) for hydrolysis of MG^+ in CTAB/1-butanol/heptane/water reverse micelles at several w , plotted as a function of $[CTAB]_0$. $[MG^+]_L = 8.65 \times 10^{-4} mol L^{-1}$, pH = 11 at 298 K.

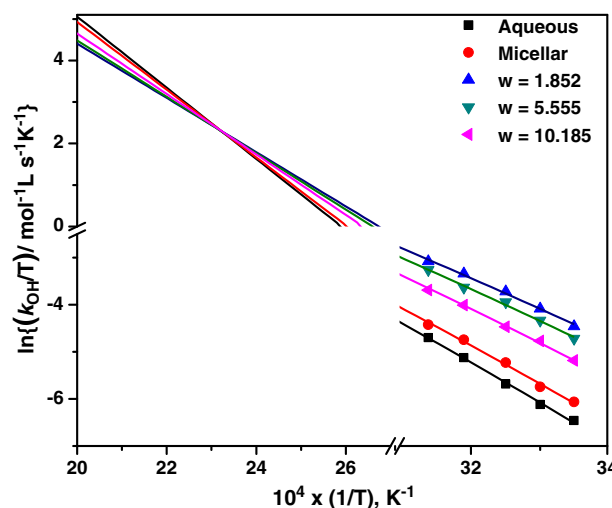


Fig. 9. Plots of $\ln\{(k_{OH}/T)/mol^{-1} L s^{-1} K^{-1}\}$ versus $(1/T)$ for alkaline hydrolysis of MG^+ in different environments. $[MG^+]_0 = 5.77 \times 10^{-5} mol L^{-1}$, pH = 11.

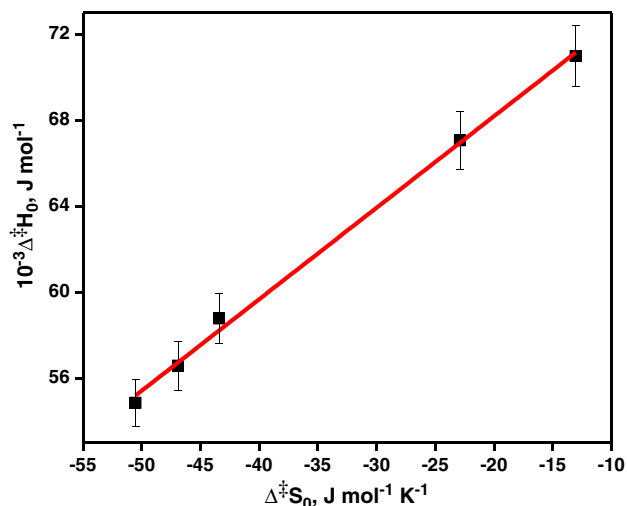


Fig. 10. Plot of $\Delta^{\ddagger}H^{\ddagger}_0$ versus $\Delta^{\ddagger}S^{\ddagger}_0$ for alkaline hydrolysis of MG^+ .

This behavior is called the compensation effect [52]. The slope of the curve has been found to be 425.9 K (± 2 K) which is very much close to that obtained from the intersection point of Fig. 9. Hence, an iso-kinetic relationship for the series of reactions may be said to exist which indicates that the alkaline hydrolysis of malachite green in different environments proceeds through an identical mechanism.

4. Conclusion

CTAB influences the kinetics of alkaline hydrolysis of malachite green (MG^+) below and above its CMC. In pre-micellar region, formation of small sub-micellar aggregates by the CTAB monomers increases rate slightly whereas in post-micellar region, the rate increases significantly for the micellar surface catalytic effect. The kinetically determined CMC of CTAB at buffered of pH = 11 has been found to be ~25% lesser than the same determined tensiometry in pure water. The rate of the reaction is noticeably dependent on the polarity at the micellar interface. The gradual increment of aggregation numbers of CTAB micelles with its concentration ensures the enhancement of the reaction rate with CTAB concentration. The kinetic behavior of the reaction in reverse micelles has been explained by considering the formalism of pseudo phase to reverse micelles where the substrate is supposed to be distributed between the interface and the water pool. Thus this alkaline fading reaction in CTAB reverse micelles takes place at much faster rate than in normal micelles or in continuous aqueous medium. The reaction rate in reverse micelles decreases with increasing water pool size. The activation parameters of the reaction corroborate the kinetic data, and indicate an iso-kinetic relationship for the reaction going on in different environments. Thus the above experimental findings reveal that CTAB reverse micelle gives us a more efficient route for the removal of malachite green from waste water in the textile industry in a much economic approach.

Acknowledgment

S D acknowledges the University Grants Commission (UGC), New Delhi, for junior research fellowship and A.K. acknowledges the Council

of Scientific and Industrial Research (CSIR), New Delhi, for the senior research fellowship.

References

- J. Li, Y. Qiao, Y. Wei, *J. Anal. Chem.* 27 (1999) 1072–1075.
- M. Golzio, J. Teissie, M.P. Rols, *Proc. Natl. Acad. Sci. U. S. A.* 99 (2002) 1292.
- A. Hagfeldt, G. Boschloo, L. Sun, L. Kloo, H. Pettersson, *Chem. Rev.* 110 (2010) 6595–6663.
- H. Zollinger, *Color chemistry: Syntheses, Properties and Applications of Organic Dyes and Pigments*, VCH Publishers, Weinheim, 1991.
- H. Zhiqiao, L. Lili, S. Shuang, X. Min, X. Lejin, Y. Haiping, C. Jianmeng, *Sep. Purif. Technol.* 62 (2008) 376–381.
- S. Nilratnisakorn, P. Thiravetyan, W. Nakbanpote, *Sci. Total Environ.* 384 (2007) 67–76.
- L.S. Andrade, L.A.M. Ruotolo, R.C. Rocha-Filho, N. Bocchi, S.R. Biaggio, J. Iniesta, V. Garcia-Garcia, V. Montiel, *Chemosphere* 66 (2007) 2035–2043.
- F. Robina, R. Faiza, B. Sofia, S. Maria, K. Sajjad, F. Umar, R. Abdur, F. Ather, P. Arshed, M. al Hassan, *S.F. Shaikat, World Appl. Sci. J.* 6 (2009) 234–237.
- F. Robina, L.F. Kai, S.F. Shaikat, J.J. Huang, *J. Environ. Sci.* 5 (2003) 710–714.
- W.R. Mabey, T. Mill, *J. Phys. Chem.* 7 (1978) 383–415.
- C.A. Bunton, L.S. Romsted, in: P. Kumar, K.L. Mittal (Eds.), *Handbook of Microemulsion Science and Technology*, Marcel Dekker, New York, 1999.
- C.A. Bunton, J. Yao, L.S. Romsted, *Curr. Opin. Colloid Interface Sci.* 2 (1997) 622–628.
- L.S. Romsted, in: K.L. Mittal, B. Lindman (Eds.), *Surfactants in Solution*, Plenum Press, New York, 1984.
- J.H. Fendler, E.J. Fendler, *Catalysis in Micellar and Macromolecular Systems*, Academic Press, New York, 1975.
- S.K. Ghosh, S. Kundu, M. Mandal, T. Pal, *Langmuir* 18 (2002) 8756–8760.
- S. Nath, S.K. Ghosh, S. Panigrahi, T. Pal, *Colloids Surf., A* 244 (2004) 31–37.
- L.G. Qiu, A.J. Xie, Y.H. Shen, *Colloid Polym. Sci.* 283 (2005) 1343–1348.
- F.M. Menger, C.E. Portnoy, *J. Am. Chem. Soc.* 89 (1967) 4698–4703.
- K. Ruan, Z. Zhao, J. Ma, *Colloid Polym. Sci.* 279 (2001) 813–818.
- K. Martinek, I.V. Berezin, Y.L. Khmelnskiy, N.L. Klyachko, A.V. Levashov, *Czech. Chem. Commun.* 52 (1987) 2589–2602.
- F.P. Cavasino, C. Sbriziolo, M.L. Turco Liveri, *J. Phys. Chem. B* 102 (1998) 5050–5054.
- S. Adhikari, R. Joshi, C. Gopinathan, *Int. J. Chem. Kinet.* 30 (1998) 699–705.
- H.K. Mandal, T. Majumdar, A. Mahapatra, *Int. J. Chem. Kinet.* 43 (2011) 579–589.
- L.Y. Zakharovaa, A.R. Ibragimovaa, F.G. Valeeva, L.A. Kudryavtseva, A.I. Konovalova, S.N. Shtykovb, L.S. Shtykovab, I.V. Bogomolova, *J. Mol. Liq.* 116 (2005) 83–91.
- L.Y. Zakharova, A.R. Ibragimova, F.G. Valeeva, L.A. Kudryavtseva, *Russ. J. Phys. Chem.* A 81 (2007) 23–27.
- P.L. Luisi, L.J. Magid, J.H. Fendler, *Crit. Rev. Biochem.* 20 (1986) 409–475.
- K.F. Thompson, L.M. Gierasch, *J. Am. Chem. Soc.* 106 (1984) 3648–3652.
- M.J. Politi, H. Chaimovich, *J. Phys. Chem.* 90 (1986) 282–287.
- S. Barbaric, P.L. Luisi, *J. Am. Chem. Soc.* 103 (1981) 4239–4244.
- S.S. Tang, G.G. Chang, *J. Org. Chem.* 60 (1995) 6183–6185.
- S. Piera-Velazquez, F. Marhuenda-Egea, E. Cadenas, *J. Mol. Catal. B Enzym.* 13 (2001) 49–55.
- D.F. Duxbury, *Chem. Rev.* 93 (1993) 381–433.
- C.A. Bunton, N. Carrasco, S.K. Huang, C.H. Paik, L.S. Romsted, *J. Am. Chem. Soc.* 100 (1978) 5420–5425.
- C.D. Ritchie, D.J. Wright, D.S. Huang, A.A. Kamego, *J. Am. Chem. Soc.* 97 (1975) 1163–1170.
- F.J. Green, *The Sigma-Aldrich Handbook of Stains, Dyes and Indicators*, Aldrich Chemical Company, Inc., Milwaukee, Wisconsin, 1990.
- A. Dan, I. Chakraborty, S. Ghosh, S.P. Moulik, *Langmuir* 23 (2007) 7531–7538.
- K. Kalyanasundaram, J.K. Thomas, *J. Am. Chem. Soc.* 99 (1977) 2039–2044.
- D.R. Lide, *CRC Handbook of Chemistry and Physics*, CRC Press, Boca Raton, FL, 1992.
- A. Malliaris, J. Lang, R. Zana, *J. Chem. Soc., Faraday Trans. 1* 82 (1986) 109–118.
- M. Almgren, J.E. Lofroth, *J. Colloid Interface Sci.* 81 (1981) 486–492.
- A.K.M. Shafiq Ullah, I. Kamal, *BRAC Univ. J.* 4 (2007) 59–62.
- S. Javadian, V. Ruhi, A. Heydari, A. Asadzadeh Shahir, A. Yousefi, J. Akbari, *Ind. Eng. Chem. Res.* 52 (2013) 4517–4526.
- Z. Yuanqin, Z. Xiancheng, Y. Xiaoqi, T. Anming, *J. Dispers. Sci. Technol.* 20 (1999) 437–448.
- C. Berberidou, I. Poulous, N.P. Xekoukoulotakis, *Appl. Catal. B Environ.* 74 (2007) 63–72.
- G.G. Warr, D.F. Evans, *Langmuir* 4 (1988) 217–224.
- E.D. Hughes, *Trans. Faraday Soc.* 37 (1941) 603–631.
- C.K. Ingold, *Structure and Mechanism in Organic Chemistry*, Bell, London, 1993.
- O. Soriyan, O. Owuyomi, A. Ogunniyi, *Acta Chim. Slov.* 55 (2008) 613–616.
- M.L. Moya, C. Izquierdo, J. Casado, *J. Phys. Chem.* 95 (1991) 6001–6004.
- M. Belletete, G. Durocher, *J. Colloid Interface Sci.* 134 (1990) 289–293.
- P.W. Atkins, J.D. Paula, *Physical Chemistry*, Oxford University Press, New York, 2002.
- L. Liu, Q.X. Guo, *Chem. Rev.* 101 (2001) 673–695.